

On Integrability and Chaos in Discrete Systems

Mark J. Ablowitz

Department of Applied Mathematics
University of Colorado-Boulder
Boulder, Colorado, 80309, USA

Yasuhiro Ohta

Department of Applied Mathematics,
Faculty of Engineering, Hiroshima University
1-4-1 Kagamiyama, Higashi-Hiroshima 739, Japan

A. David Trubatch

Department of Applied Mathematics
University of Colorado-Boulder
Boulder, Colorado, 80309, USA

Abstract

The scalar nonlinear Schrödinger (NLS) equation and a suitable discretization are well known integrable systems which exhibit the phenomena of “effective” chaos. Vector generalizations of both the continuous and discrete system are discussed. Some attention is directed upon the issue of the integrability of a discrete version of the vector NLS equation.

1 Introduction

Integrable systems are usually thought to demonstrate regular temporal and spatial evolution. Philosophically, it seems to be pleasing to separate integrable motion from chaotic dynamics. The latter being the “opposite” of the former. However, upon more careful investigation, there is not such a simple distinction. Many well known integrable systems are actually “on the verge” of exhibiting chaos whereby any perturbation: physical, or numerical—e.g. even roundoff effects, can push them “over the edge” and thereby excite chaotic dynamics. In one dimension, the classical pendulum is such an example. And in one space - one time dimension the well known integrable systems: the sine-Gordon and nonlinear Schrödinger equations with periodic boundary values are examples of integrable systems where complex and irregular dynamics can be excited in certain regions of phase space [1, 3, 6, 7]. The common feature in such situations is an initial value prescribed in the proximity of special regimes of phase space, referred to as homoclinic manifolds. Homoclinic manifolds are locations in phase space in which highly sensitive solution structures exist. We have, in earlier papers, discussed the notion of “effective” chaos [3, 6] whereby any perturbation can excite irregular and unstable motion—both of which are manifestations of chaotic dynamics.

Chaotic behavior in perturbed integrable systems is significant for two reasons: (i) Numerical schemes can be considered as perturbations of the original system. If the perturbation of the numerical scheme introduces chaos, the results of simulations will not reflect the dynamics of the unperturbed system. (ii) In physical applications, perturbations—from effects neglected in the derivation of the integrable equation—can induce chaotic behavior in the system. Even if this effective chaos is only present in certain regions of phase space, it is, in general, impossible to determine *a priori* where these regions are.

Finite-difference discretizations of integrable PDE’s can be considered both as perturbations of the original PDE and as the basis for numerical schemes. Here, we will consider spatial finite-difference schemes.

These finite-difference discretizations can be integrated in time by well-known, highly-accurate methods for integrating ordinary differential equations. Numerical schemes based on finite differences are useful because, unlike spectral schemes, finite-difference schemes do not require special boundary conditions.

We begin by first discussing the scalar nonlinear Schrödinger equation (NLS):

$$iq_t = q_{xx} + 2q|q|^2. \quad (1)$$

NLS is integrable via the inverse scattering transform (IST) and has significant applications in physics, such as the evolution of small amplitude slowly varying wave packets in: deep water, nonlinear optics and plasma physics (see e.g. [8]).

Many discretizations of NLS have physical applications as discrete systems (see e.g. [9, 10, 13, 14]). In particular, consider two conservative (in fact, Hamiltonian) finite-difference discretizations of NLS, the diagonal discrete NLS (DDNLS),

$$i\frac{d}{dt}q_n = \frac{1}{h^2}(q_{n-1} - 2q_n + q_{n+1}) + 2|q_n|^2q_n \quad (2)$$

and the integrable discrete NLS (IDNLS),

$$i\frac{d}{dt}q_n = \frac{1}{h^2}(q_{n-1} - 2q_n + q_{n+1}) + |q_n|^2(q_{n+1} + q_{n-1}). \quad (3)$$

These two systems differ only in the discretization of the nonlinear term, yet they have very different properties. While both these discretizations retain the Hamiltonian structure of the PDE, IDNLS (3) is integrable via the IST [4] while DDNLS is not. Differences in the dynamics of these two systems shed light on the role of integrability in the development of chaos in perturbations. In fact, these two schemes can exhibit very different responses to the same initial data. In the case of periodic boundary conditions, the onset and structure of “effective” chaos is very different between (2) and (3) while, for the infinite lattice with a rapidly-decaying boundary condition, (3) has solitons and (2) does not. The affect of non-conservative perturbations to NLS has also been considered in the literature (e. g. [17]), but we will not do so here.

The vector generalization of NLS,

$$i\mathbf{q}_t = \mathbf{q}_{xx} + 2\|\mathbf{q}\|^2\mathbf{q} \quad (4)$$

where \mathbf{q} is an N -component vector and $\|\cdot\|$ denotes the vector norm, can be integrated via the IST and has soliton solutions [16] (actually, in [16] only the case $N = 2$ was studied in detail; however the extension to the N -th order vector system is straightforward).

Vector NLS (eq. 4, hereafter referred to as VNLS) is applicable, physically, under the similar conditions as NLS (1) with the generalization that the field can have more than one nontrivial component. For example, in optical fibers, the two components of the second-order ($N = 2$) VNLS correspond to components of the electric field transverse to the direction of wave propagation. These components of the transverse field compose a basis of the polarization states (we note that, in general, a non-integrable variation of VNLS is the appropriate model for optical fibers [18], however, in certain circumstances (4) is indeed the appropriate equation [19, 11]).

Although certain perturbations of the integrable VNLS have been investigated [15, 21], the question of effective chaos in VNLS has not been studied. Discretizations of VNLS are natural candidates for the study of chaos induced by perturbations. The research on effective chaos for NLS suggests that the results of such studies will depend strongly on the choice of discretization, particularly in the discretization of the nonlinear term. Therefore, the choice of discretization for VNLS merits closer analysis.

The system

$$i\frac{d}{dt}\mathbf{q}_n = \frac{1}{h^2}(\mathbf{q}_{n-1} - 2\mathbf{q}_n + \mathbf{q}_{n+1}) + \|\mathbf{q}_n\|^2(\mathbf{q}_{n-1} + \mathbf{q}_{n+1}) \quad (5)$$

where \mathbf{q}_n is an N -component vector, manifests properties of an integrable system (cf. Section 5). Moreover, this system (5) is extremely useful as a numerical scheme for VNLS (4). Therefore, the underlying chaotic nature of some periodic solutions of (4) and (5) can be examined effectively. Because (5) is a natural generalization of IDNLS (3) that has some important symmetries of VNLS, we refer to this system as the symmetric discretization of VNLS or, simply the symmetric system.

To date, no compatible linear operator scattering pair for the symmetric system (5) has been derived. Without such a pair (5) cannot be solved via the IST. However, under the reduction $\mathbf{q}_n = e^{i\omega t} \mathbf{v}_n$, where \mathbf{v}_n is independent of t , (5) reduces to an N -dimensional difference equation which is known to be integrable (cf. [22]). Also, we note that the reduction $\mathbf{q}_n = \mathbf{c}q_n$, where \mathbf{c} is a constant complex unit vector ($\|\mathbf{c}\| = 1$) and q_n a scalar, (5) reduces to the integrable discretization of NLS (3).

The symmetric discretization (5) has a class of analytical multi-soliton solutions [5, 20]. These exact solutions of the symmetric system only reduce to a subset of those associated with (4). In order to determine whether general multi-soliton solutions exist, we examined, by numerical simulation, the interactions of solitary waves associated with the symmetric system which lie outside this class of known analytical solutions. The numerical evidence, discussed later in this paper, indicates that, in the symmetric system, the solitary waves interact elastically and are therefore true solitons. This finding strongly suggests that the symmetric system (5) is indeed integrable.

In the future, we shall identify regions of phase space where effective chaos could be expected for the symmetric system. In these regions of phase space, the dynamics of the symmetric discretization can be compared, by numerical simulation, to the dynamics of different discretizations of VNLS—e.g. replacing the nonlinear term in (4) by $\|\mathbf{q}_n\|^2 \mathbf{q}_n$ in analogy with (2).

2 Effective Chaos in NLS

Let us return briefly to the scalar equation (1). In both discretizations (2,3), truncation error is $O(h^2)$. For the non-integrable discretization (2) the truncation error is a perturbation from integrability while the integrable discretization (3) is, as its name implies, integrable for finite h . For NLS with periodic initial data, some initial conditions evolve irregularly in space and time when numerically integrated via DDNLS (2) at moderate discretizations. At high levels of discretization this irregularity disappears though often very slowly. This “chaotic” response is due to the perturbation from integrability in the truncation error in DDNLS (2), the non-integrable discretization. Simulations with IDNLS (3) and the same initial data do not show irregularity even at moderate levels of discretization [1, 12].

Irregular and chaotic dynamics can also be caused by perturbations due to round-off error in the floating point arithmetic of computer simulation. This is demonstrated by integrating the initial data with the integrable discretization (3) via the *mathematically* equivalent discretization

$$i \frac{d}{dt} \tilde{q}_n = \frac{1}{h^2} (\tilde{q}_{n-1} - 2\tilde{q}_n + \tilde{q}_{n+1}) + |\tilde{q}_n|^2 q_{n+1} + |\tilde{q}_n|^2 \tilde{q}_{n-1}. \quad (6)$$

The only difference between the discretizations (3) and (6) is the distribution of the multiplication in the nonlinear term. Nonetheless, in numerical simulations, the two solutions, $q_n(t)$ and $\tilde{q}_n(t)$, with the same initial data ($q_n(0) = \tilde{q}_n(0)$) can dramatically drift apart until their difference is comparable to the amplitudes of the solution [6, 7].

These instances of chaotic behavior in NLS are associated with proximity of the initial data to homoclinic manifolds of NLS. The location and structure of these homoclinic manifolds can be determined for NLS by the spectral theory of the associated linear scattering problem. When initial data are chosen well away from the homoclinic manifolds, the chaotic responses described above are observed only at coarser discretizations or not at all [2, 7]. In low dimensional systems, chaotic dynamics in regions of phase space are associated with crossings of the homoclinic manifold. However, by analyzing the spectral data of the associated linear problem, one can demonstrate that for DDNLS, chaotic dynamics generically occur without the solution crossing the homoclinic manifold [3].

3 Vector NLS

Solutions of VNLS (4) are more complex than those of the scalar case (1) because there are more degrees of freedom. In particular, the dynamics of soliton interactions depends on the vector nature of the system. A clear definition of solitons in the vector system is a prerequisite for analyzing soliton solutions in the discretizations of VNLS such as the symmetric system (5). Hence, here, we give a brief account of some key properties of VNLS and their affect on the soliton solutions.

Under the reduction

$$\mathbf{q} = \mathbf{c}q \quad (7)$$

where \mathbf{c} is a constant, N -component vector such that $\|\mathbf{c}\|^2 = 1$ and q is a scalar function of x and t , vector NLS (4) reduces to NLS (1). This is a manifestation of the fact that the vector system (4) is a generalization of NLS. When the vector-valued independent variable \mathbf{q} is restricted to a one-dimensional subspace (which is equivalent to a scalar), NLS is recovered. As a consequence, any solution of scalar NLS has a corresponding family of solutions of VNLS. We call a solution of the form (7) a *reduction solution*. We refer to \mathbf{c} as the *polarization* of the reduction solution.

The solitons of VNLS can be found by IST for the boundary condition of rapid decay on the whole line [16]. The one-soliton solutions of VNLS are the reduction solutions (i.e. in the form of eq. 7) in which the scalar function q is a one-soliton solution of NLS and \mathbf{c} can be any unit vector. In the backward ($t \rightarrow -\infty$) and forward ($t \rightarrow +\infty$) long-time limits, a generic rapidly-decaying whole-line solution of VNLS asymptotically approaches a linear superposition of solitons:

$$\mathbf{q} \sim \sum_j \mathbf{q}_j^\pm \quad \text{as } t \rightarrow \pm\infty$$

where $\mathbf{q}_j^\pm = \mathbf{c}_j^\pm q_j^\pm$, \mathbf{c}_j^\pm is a complex unit vector and q_j^\pm is a one-soliton solution of NLS such that q_j^+ has the same amplitude and speed as q_j^- [16]. Therefore, in the long-time limits, we can define a separate polarization vector for each soliton, namely \mathbf{c}_j^\pm . Comparison of the forward (+) and backward (-) long-time limits shows that, in general,

$$\mathbf{c}_j^- \neq \mathbf{c}_j^+.$$

The polarization of each individual soliton shifts due interaction with the other solitons. However,

$$\|\mathbf{c}_j^+\|^2 = \|\mathbf{c}_j^-\|^2 = 1. \quad (8)$$

In addition to the shift in the polarization, the locations of individual soliton peaks are shifted by the interaction with other solitons (this is the usual phase shift seen in scalar soliton equations). A closed formula for these phase shifts (the change in polarization and in the location of the peak) can be derived via the IST [16].

We refer to the squared absolute value of a component of the polarization vector as the *intensity* of that component of the polarization. The intensity of the ℓ -th component of the j -th soliton is given by $|c_j^{(\ell)+}|^2$ ($|c_j^{(\ell)-}|^2$) where $c_j^{(\ell)+}$ ($c_j^{(\ell)-}$) is the ℓ -th component of \mathbf{c}_j^+ (\mathbf{c}_j^-), the polarization vector of j -th soliton in the forward (backward) long-time limit. The relation (8) implies that, for each soliton, the sum of the intensities is constant, namely equal to one. However, the distribution of the intensity among the components of each soliton will not, in general, be equal in the forward and backwards long-time limits due to interaction with other solitons: that is, subject to the constraint of eq. (8), in general,

$$|c_j^{(\ell)-}|^2 \neq |c_j^{(\ell)+}|^2. \quad (9)$$

This shift in the distribution of intensity between the backward and the forward long-time limits (9) is a distinctive feature of soliton interactions in the vector system (4). There is no corresponding phenomenon in the scalar equation (1).

Manakov [16] showed by IST that the following special case holds for M -soliton solutions: if, for any $j, k = 1 \dots M$, either

$$|\mathbf{c}_j^- \cdot \mathbf{c}_k^-| = 1 \quad (10a)$$

or

$$|\mathbf{c}_j^- \cdot \mathbf{c}_k^-| = 0, \quad (10b)$$

where \cdot denotes the inner product, then it turns out that

$$|\mathbf{c}_j^- \cdot \mathbf{c}_j^+| = 1 \quad (11)$$

and, moreover,

$$|c_j^{(\ell)-}|^2 = |c_j^{(\ell)+}|^2 \quad (12)$$

for all $\ell = 1, 2, j = 1, \dots, M$ (we assume the case of two components). These soliton solutions constitute a special class of vector solitons where the distribution of intensity of an individual soliton is not shifted (i.e. the relation (12) holds) even though the solitons pass through each other.

When considered as a model for electromagnetic wave propagation in optical fibers, the components of VNLS (4) play the role of a basis for the polarization vector of the transverse electric field. Because this choice of basis is arbitrary, the vector system (4) ought to be, and is, invariant under a change of basis. Mathematically, a change of basis is obtained by the independent-variable transformation

$$\hat{\mathbf{q}} = \mathbf{U}\mathbf{q} \quad (13)$$

where \mathbf{U} is a unitary matrix. The new independent variable, $\hat{\mathbf{q}}$, satisfies VNLS if, and only if, \mathbf{q} does. We note that, in particular, the distribution of intensity for a soliton depends on the choice of basis. However, the conditions (10a-10b) and the consequence (11) are independent of the choice of basis—i. e. dot products are preserved under unitary transformations.

4 Discretization of Vector NLS

As we noted previously, the symmetric system (5) is the natural vector generalization of IDNLS (3). However, the most natural vector generalization of the linear scattering pair for IDNLS yields the following nonlinear equation as a result of compatibility:

$$i \frac{d}{dt} \mathbf{q}_n = \frac{1}{h^2} (\mathbf{q}_{n-1} - 2\mathbf{q}_n + \mathbf{q}_{n+1}) - (\mathbf{r}_n^T \mathbf{q}_{n-1}) \mathbf{q}_n - (\mathbf{r}_n^T \mathbf{q}_n) \mathbf{q}_{n+1} \quad (14a)$$

$$-i \frac{d}{dt} \mathbf{r}_n = \frac{1}{h^2} (\mathbf{r}_{n-1} - 2\mathbf{r}_n + \mathbf{r}_{n+1}) - (\mathbf{r}_n^T \mathbf{q}_n) \mathbf{r}_{n-1} - (\mathbf{r}_{n+1}^T \mathbf{q}_n) \mathbf{r}_n \quad (14b)$$

where \mathbf{q}_n is an N -component vector as is \mathbf{r}_n and the superscript T denotes the transpose. To get VNLS from (14a-14b), we take $\mathbf{r} = -\mathbf{q}^*$ (* denotes the complex conjugate) after taking the continuum limit. The discrete system (14a-14b) does not admit the symmetry $\mathbf{r}_n = -\mathbf{q}_n^*$ for finite h . Hence, we refer to (14a-14b) as the asymmetric discretization of VNLS, or more briefly as the asymmetric system. We emphasize that (14a-14b) is not equivalent to the symmetric system (5).

The asymmetric system has a class of soliton solutions which corresponds to all the soliton solutions of the continuous version of VNLS (4) [5]. However, in these solutions, $|\mathbf{r}_n - (-\mathbf{q}_n^*)| = O(h)$ so the asymmetry cannot not be ignored [5]. In general, for initial data such that $\mathbf{r}_n = -\mathbf{q}_n^*$, the solution will evolve so that $\mathbf{r}_n \neq -\mathbf{q}_n^*$ at later times. The unavoidable asymmetry of the asymmetric system (14a-14b) makes it less desirable as a discretization of VNLS. Hence, we turn our attention to the symmetric discretization.

We now discuss some important properties of the symmetric discretization. The symmetric system (5) reduces to IDNLS (3) under the reduction

$$\mathbf{q}_n = \mathbf{c}q_n \quad (15)$$

where \mathbf{c} is a constant vector such that $\|\mathbf{c}\| = 1$. This is the discrete analog of eq. (7). As for VNLS, we refer to the vector \mathbf{c} in (15) as the *polarization* of the *reduction solution* \mathbf{q}_n . Also, the symmetric system is invariant under a discrete version of the independent-variable transformation (13). Hence, as for the PDE (4), the components of \mathbf{q}_n can be considered to be a basis of the polarization and the discrete form of the unitary transformation (13) as a change of coordinates. Perhaps the most important property of the symmetric system is the existence of soliton solutions. These are discussed in the next section.

5 Soliton Solutions of the Symmetric System

In order to demonstrate the existence of solitons in the symmetric system, we must first identify the appropriate vector solitary waves. Given these solitary wave solutions, we then investigate their interaction. To construct a vector solitary-wave solution of the symmetric system (5) multiply the scalar one-soliton solution of IDNLS (3) by an arbitrary unit vector. The resulting vector solution \mathbf{q}_n is the reduction solution— i.e. of the form (15) —where the scalar function q_n is given by:

$$q_n(t) = Ae^{-i(bhn - \omega t - \phi)} \text{sech}(ahn - vt - \theta) = e^{i\phi} \hat{q}_n(t) \quad (16)$$

with

$$A = \frac{\sinh(ah)}{h}, \quad \omega = \frac{2(1 - \cosh(ah) \cos(bh))}{h^2}, \quad v = 2 \frac{\sinh(ah) \sin(bh)}{h^2}$$

where a, b, θ, ϕ are arbitrary parameters. For this vector solitary wave, a and b determine the amplitude, A and speed, v . The parameter θ is the position of the peak of $\|\mathbf{q}\|$ at $t = 0$ and ϕ is an overall complex phase.

The simplest example of the interaction of these vector solitary waves is constructed from the scalar M -soliton solution of IDNLS. Let $q_{j,n}$ be the scalar M -soliton solution of IDNLS with parameters a_j, b_j and consider the vector solution $\mathbf{q}_n = \mathbf{c}q_n$ where, as before, \mathbf{c} is a unit vector. Then in the long-time limits ($t \rightarrow \pm\infty$),

$$\mathbf{q}_n^\pm \sim \mathbf{c} \sum_{j=1}^M e^{i\phi_j^\pm} \hat{q}_{j,n}^\pm, \quad (17)$$

where $\hat{q}_{j,n}^\pm$ is a solitary-wave solution of the form given above in eq. (16) with $a = a_j, b = b_j, \theta = \theta_j^\pm$. The parameters ϕ_j^\pm are complex phase shifts of the scalar soliton interaction. For such a solution, each solitary wave envelope can be thought of as having an individual polarization:

$$\mathbf{c}_j^\pm = \mathbf{c} e^{i\phi_j^\pm}.$$

In this example, we see that each of the vector solitary waves has the same amplitude and speed in the forward long-time limit as it had in the backward long-time limit (i.e. a soliton-type interaction). This

suggests that the individual vector solitary waves constructed from (16) are, in fact, the solitons of the symmetric system (5).

However, in this simple example (15), since \mathbf{c} is the same for each solitary wave, the polarizations of the vector solitary waves must satisfy

$$|\mathbf{c}_j^- \cdot \mathbf{c}_k^-| = 1$$

for all $j, k = 1 \dots M$. There is no such constraint for the solitons in the vector PDE (4). Therefore, we investigate the more general vector solitary-wave interactions (i.e. $|\mathbf{c}_j^- \cdot \mathbf{c}_k^-| < 1$) in the discrete symmetric system by direct and numerical methods.

5.1 Soliton solutions by Hirota's Method

To find soliton solutions of the symmetric system (5) by Hirota's method we write it in the bilinear form: by taking

$$\mathbf{q}_n = \frac{\mathbf{g}_n}{f_n}.$$

where \mathbf{g}_n is a vector and f_n is a scalar, we find

$$ih^2 D_t f_n \cdot \mathbf{g}_n = f_{n-1} \mathbf{g}_{n+1} f_{n-1} - 2f_n \mathbf{g}_n + f_{n+1} \mathbf{g}_{n-1} \quad (18a)$$

$$f_{n+1} f_{n-1} - f_n^2 = h^2 \|\mathbf{g}_n\|^2 \quad (18b)$$

A two-soliton of the symmetric system is given by the following solution of the bilinear equations (18a-18b):

$$f_n = 1 + e^{\eta_{1,n} + \eta_{1,n}^*} + e^{\eta_{2,n} + \eta_{2,n}^*} + |B_1|^2 e^{\eta_{1,n} + \eta_{1,n}^* + \eta_{2,n} + \eta_{2,n}^*} \quad (19a)$$

$$g_n^{(1)} = \frac{1}{h} \left(e^{hp_1} - e^{-hp_1^*} \right) e^{\eta_{1,n}} \left(1 + B_1 e^{\eta_{2,n} + \eta_{2,n}^*} \right) \quad (19b)$$

$$g_n^{(2)} = \frac{1}{h} \left(e^{hp_2} - e^{-hp_2^*} \right) e^{\eta_{2,n}} \left(1 + B_2 e^{\eta_{1,n} + \eta_{1,n}^*} \right) \quad (19c)$$

where $g_n^{(k)}$ is the k -th component of \mathbf{g}_n and

$$\eta_{j,n} = p_j n h + \frac{i}{h^2} (2 - e^{hp_j} - e^{-hp_j}) t. \quad (20)$$

The coefficients B_j are

$$B_1 = \frac{(e^{hp_1} - e^{hp_2})(e^{hp_1} + e^{hp_2^*})}{(e^{h(p_1+p_2)} + 1)(e^{h(p_1+p_2^*)} - 1)}, \quad B_2 = -\frac{(e^{hp_1} - e^{hp_2})(e^{hp_1^*} + e^{hp_2})}{(e^{h(p_1+p_2)} + 1)(e^{h(p_1^*+p_2)} - 1)}$$

and the complex constants $p_j = a_j - ib_j$ (where $a_j > 0$ and $j = 1, 2$) determine the amplitudes and envelope speeds of the solitons.

In order to see that the above solution (19a-19c) indeed gives a two-soliton solution, consider the long-time limits (i.e. $t \rightarrow \pm\infty$). In the forward ($t \rightarrow +\infty$) and backward ($t \rightarrow -\infty$) long-time limits, this solution (19a-19c) asymptotically approaches the form

$$\mathbf{q}_n^\pm \sim \mathbf{q}_{1,n}^\pm + \mathbf{q}_{2,n}^\pm$$

where $\mathbf{q}_{j,n}^\pm = \mathbf{c}_j^\pm \hat{q}_{j,n}^\pm$ and $j = 1, 2$. The vectors \mathbf{c}_j^\pm are unit vectors and the scalars $\hat{q}_{j,n}$ are solitary waves of the form (16) with $a = a_j$, $b = b_j$ and $\theta = \theta_j^\pm$ where $j = 1, 2$. If, without loss of generality, we assume that a_j and b_j are such that $\sinh(a_1 h) \sin(b_1 h) > \sinh(a_2 h) \sin(b_2 h)$ then

$$\theta_1^- = 0, \quad \theta_1^+ = -\log |B_1|, \quad \theta_2^- = -\log |B_2|, \quad \theta_2^+ = 0$$

and

$$\mathbf{c}_1^\pm = \left(e^{i\phi_1^\pm}, 0 \right), \quad \mathbf{c}_2^\pm = \left(0, e^{i\phi_2^\pm} \right)$$

where

$$\phi_1^- = hb_1, \quad \phi_1^+ = hb_1 + \arg B_1, \quad \phi_2^- = hb_2 + \arg B_2, \quad \phi_2^+ = hb_2.$$

The two-soliton solution (19a-19c) does not encompass the most general case because

$$\mathbf{c}_1^- \cdot \mathbf{c}_2^- = 0 \tag{21a}$$

and

$$\mathbf{c}_1^+ \cdot \mathbf{c}_2^+ = 0. \tag{21b}$$

This solution can be multiplied by a unitary matrix (the discrete analog of the transformation in eq. 13) to obtain a two-soliton solution with any pair of vectors such that (21a) holds (under such a transformation, (21b) will still hold). Therefore two-soliton solutions given by (19a-19c) are a restricted class of two-soliton solutions (where eq. (21a-21b) constitutes the restriction).

For more than two solitons, Hirota's method can still be applied. The M -soliton solutions of the symmetric system take on a considerably more complicated form; they can be represented as ratios of Pfaffians [20]. Still, for these M -soliton solutions, either

$$|\mathbf{c}_j^- \cdot \mathbf{c}_k^-| = 1 \tag{22a}$$

or

$$|\mathbf{c}_j^- \cdot \mathbf{c}_k^-| = 0 \tag{22b}$$

and $|\mathbf{c}_j^- \cdot \mathbf{c}_k^+| = 1$ for $j, k = 1 \dots M$ [20, 5].

Even though analytical formulae exist for multi-soliton solutions of the symmetric system (with any number, M , of solitons), these solutions are constrained to satisfy (22a-22b). Such solutions are more general, but are like the special class of soliton solutions of the PDE discussed at the end of Section 3. They satisfy the restriction (21a-21b).

5.2 General Soliton Interactions by Numerical Simulation

Recall that, in the PDE (4), the polarizations of the individual solitons in the multi-soliton solutions (derived by IST) are not constrained—i.e there are vector multi-soliton solutions of the PDE for which the polarizations satisfy $0 < |\mathbf{c}_j^- \cdot \mathbf{c}_k^-| < 1$ for some j, k . For the discrete symmetric system (5), we investigated the general solitary-wave interaction—i.e $0 < |\mathbf{c}_j^- \cdot \mathbf{c}_k^-| < 1$ by numerical simulation because, to date, there are no analytical formulae covering this general case. Moreover, it is important to determine whether eq. (5) is integrable. The existence of general soliton solutions would strongly support the possibility that (5) is indeed

integrable. In addition, as we shall show, the measurement of soliton parameters in discrete systems requires a novel approach.

In these simulations, the initial condition was composed of vector solitary waves $\mathbf{q}_{j,n}^-$ of the form $\mathbf{q}_{j,n}^- = \mathbf{c}_j^- \hat{q}_{j,n}^-$ where the scalar $\hat{q}_{j,n}^-$ is of the form (16). In the initial condition, these vector solitary waves were well-separated. Then, the symmetric system was integrated in time by an adaptive Runge-Kutta-Merson routine (from the NAG library) until the peaks were again well-separated (see Figure 1). The separation of peaks in the initial and final conditions makes these finite-time conditions comparable to, respectively, the backwards and forwards long-time limits. In the example Figure 1, and in other simulations, the solitary waves appear to interact without any radiation or loss. We confirmed this visual result with striking quantitative measurements: we measured the difference between the solitary waves resulting from the numerical simulation and the exact solitary wave form,

$$\mathbf{q}_{j,n}^+ = \mathbf{c}_j^+ \hat{q}_{j,n}^+ \quad (23)$$

where $\hat{q}_{j,n}^+$ is of the form (16).

In order to compare the final-time data of the numerical simulation with exact solitary-wave solutions it is necessary to estimate the polarization, \mathbf{c}_j^+ , and the shift in the envelope, θ_j^+ for the j -th solitary wave at the final time (the values of \mathbf{c}_j^- , and θ_j^- are fixed by the choice of initial data). If the j -th solitary wave is actually of the form (23) at the final time, then the ℓ -th component of the vector \mathbf{c}_j^+ satisfies

$$c_j^{(\ell)+} = e^{i(b_j h n - \omega_j t_f)} \frac{q_{j,n}^{(\ell)+}}{\sqrt{|q_{j,n}^{(1)+}|^2 + |q_{j,n}^{(2)+}|^2}} \quad (24)$$

for all n where $\|\mathbf{q}_{j,n}^+\|$ is not negligible (we denote this set of points n containing the j -th solitary wave by Ω_j). In practice, we compute the estimate $\tilde{\mathbf{c}}_j^+$ by

$$\tilde{c}_j^{(\ell)+} = \text{avg}_{n \in \Omega_j} \frac{e^{i(b_j h n - \omega_j t_f)} q_n^{(\ell),f}}{\sqrt{|q_n^{(1),f}|^2 + |q_n^{(2),f}|^2}},$$

where $\ell = 1, 2$ and $(q_n^{(1),f}, q_n^{(2),f})$ is the numerical data at the final time, $t = t_f$. Similarly, if the absolute value of j -th solitary wave is a sech envelope as in (16), then for all $n \in \Omega_j$,

$$\theta_j^+ = a h n - v_j t_f - \text{sech}^{-1} \left(\frac{|q_{j,n}^{(1)+}|^2 + |q_{j,n}^{(2)+}|^2}{A_j} \right) \quad (25)$$

where $A_j = \frac{\sinh(a_j h)}{h}$. Again, we construct the estimate $\tilde{\theta}_j^+$ by taking the average of the right-hand side of (25) over $n \in \Omega_j$ where we substitute $(q_{j,n}^{(\ell)+}, q_{j,n}^{(\ell)+})$ with $(q_n^{(1),f}, q_n^{(2),f})$, the numerical data at the final time. Note that we assume that a_j and b_j do not change in the evolution and hence we do not estimate them in the forward long-time limit.

The difference between the numerically-derived solitary wave $\mathbf{q}_{j,n}^+$ and a solitary wave-form of the type (23) is measured by

$$\Delta_j = \max_{n \in \Omega_j} \frac{\|\mathbf{q}_{j,n}^f - \tilde{\mathbf{q}}_{j,n}^+\|}{A_j} \quad (26)$$

where $\mathbf{q}_{j,n}^f = (q_n^{(1),f}, q_n^{(2),f})$ for $n \in \Omega_j$ and $\tilde{\mathbf{q}}_{j,n}^+$ is the estimated soliton wave-form

$$\tilde{\mathbf{q}}_{j,n}^+ = \tilde{\mathbf{c}}_j^+ A_j e^{-i(b_j h n - \omega_j t_f)} \text{sech} \left(a_j h n - v_j t_f - \tilde{\theta}_{0,j}^+ \right).$$

In order to study the symmetric case in a parameter regime that is “far” from the continuum limit, we ran the simulations with amplitude parameters, a_j , and grid sizes h such that the soliton width was comparable to the grid size (equivalently, $a_j h \approx 1$). For the parameters b_j we considered two regimes: (i) b_j such that the spatial frequency of the complex carrier-wave $e^{ib_j n h}$ was comparable to the grid size ($b_j h \approx 1$) and (ii) b_j such that the spatial frequency was large compared to the grid size ($b_j h \approx .1$). We ran simulations with several values of a_j for each b_j . In particular, when $b_j h \approx .1$ the speed of the solitary-wave envelopes was slow, the solitary waves interacted over a long time.

The time-integration routine we used (routine D02BAF from the NAG library) is adaptive and computes until an internally-defined error tolerance reaches a user-specified value. In the simulations, when the error tolerance in the adaptive integration scheme was decreased, the difference between the data at the final time and a soliton waveform (26) decreased proportionally. Table 1 shows data from an example experiment. In this experiment, the initial data is generic in that $0 < |\mathbf{c}_1^- \cdot \mathbf{c}_2^-| = .6 < 1$ and, to date, there is no known analytical formula for the solution. The error, Δ_j , is proportional to the error tolerance of the integration. This indicates that the numerically computed solution converges to an elastic soliton interaction as the time integration is computed more accurately. We conclude from numerous such experiments that, in fact, the vector solitary waves of the form $\mathbf{q}_{j,n}^- = \mathbf{c}^- q_{j,n}^-$ (where the scalar $q_{j,n}^-$ is of the form of eq. 16) interact elastically—i. e. the vector solitary waves behave as true solitons—in the symmetric system (5).

For a generic interaction of two solitary waves of the symmetric system, $0 < |\mathbf{c}_1^- \cdot \mathbf{c}_2^-| < 1$. In the PDE (4), such generic vector soliton interactions result in the shift of the polarizations of the individual vector solitons—i.e. $|\mathbf{c}_j^- \cdot \mathbf{c}_j^+| < 1$, $j = 1, 2$. We observe the same distinctive vector behavior in numerical simulations of the discrete symmetric system. Table 2 shows the results of a number of typical experiments. In a two soliton-interaction we can always pick a basis for the polarization such that $\mathbf{c}_1^- = (1, 0)$ and $\arg c_2^{(2)-} = 0$. Because \mathbf{c}_2^- is a unit vector with two components, the absolute value of $c_2^{(2)-}$ satisfies:

$$|c_2^{(2)-}| = \sqrt{1 - |c_2^{(1)-}|^2}.$$

Hence, as in Table 2, in order to consider a general two-soliton interaction, we need only vary $c_2^{(1)-}$. In our simulations, we see the polarizations of the individual solitary waves shift due to interaction while the solitary waves retain their shape. In the example interactions tabulated in Table 2, there are initial conditions that result in large polarization shifts, that is the inner products of the forward and backward polarization of an individual vector solitary wave is small (e.g. $|\mathbf{c}_1^- \cdot \mathbf{c}_1^+| = .158$). This is the intrinsically vector-type soliton interaction of the solitary waves. Therefore, we conclude from the numerical simulations that the symmetric system displays general vector-soliton behavior analogous to VNLS, the PDE continuum limit.

We also considered the following generalization of the two-component symmetric system

$$i \frac{d}{dt} q_n^{(1)} = \frac{1}{h^2} (q_{n-1}^{(1)} - 2q_n^{(1)} + q_{n+1}^{(1)}) + (|q_n^{(1)}|^2 + B|q_n^{(2)}|^2) (q_{n-1}^{(1)} + q_{n+1}^{(1)}) \quad (27a)$$

$$i \frac{d}{dt} q_n^{(2)} = \frac{1}{h^2} (q_{n-1}^{(2)} - 2q_n^{(2)} + q_{n+1}^{(2)}) + (B|q_n^{(1)}|^2 + |q_n^{(2)}|^2) (q_{n-1}^{(2)} + q_{n+1}^{(2)}). \quad (27b)$$

In the case $|B| \neq 1$, we found very strong inelastic effects. In particular, depending on the initial soliton parameters, numerical simulations of soliton interaction, the solitons (i) produced large radiative tails and/or (ii) reflected from one another. These numerical results suggest that the general elastic interactions observed in the symmetric system (5) are a manifestation of the integrability of that system. We mention that (27a-27b) is an example of the interesting generalization of (5) where the nonlinear term for the j -th component, $(\sum_{k=1}^N |q_n^{(k)}|^2) (q_{n-1}^{(j)} + q_{n+1}^{(j)})$, is replaced by $(\sum_{k=1}^N B_{j,k} |q_n^{(k)}|^2) (q_{n-1}^{(j)} + q_{n+1}^{(j)})$. We expect that this model will exhibit a range of different inelastic effects between solitary waves such as those observed in (27a-27b).

The mechanism of the elastic soliton interactions observed for the symmetric system remains to be completely explained analytically. More generally, a proof that the symmetric system can be completely integrated remains as an important open problem.

Acknowledgments

This work was supported in part by NSF grants DMS-9404265 and DMS-9703850 as well as U. S. Air Force AASERT grant DOD AF-F49620-93-I-0574 and U. S. Navy AASERT grant DOD N00014-94-1-0915.

References

- [1] M. J. Ablowitz, S. Chakravarty, and B. M. Herbst. Integrability, computation and applications. *Acta Applicandae Mathematicae*, 39:5–37, 1995.
- [2] M. J. Ablowitz and P. A. Clarkson. *Solitons Nonlinear Evolution Equations and Inverse Scattering*. Number 149 in London Mathematical Society Lecture Note Series. Cambridge University Press, 1991.
- [3] M. J. Ablowitz, B. M. Herbst, and C. M. Schober. Computational chaos in the nonlinear Schrödinger equation without homoclinic crossings. *Physica A*, 228:212–235, 1996.
- [4] M. J. Ablowitz and J. F. Ladik. A nonlinear difference scheme and inverse scattering. *Studies in Applied Mathematics*, 55:213–229, 1976.
- [5] M. J. Ablowitz, Y. Ohta, and A. D. Trubatch. On discretizations of the vector nonlinear Schrödinger equation. APPM Preprint 349, University of Colorado-Boulder, March 1998.
- [6] M. J. Ablowitz and C. M. Schober. Effective chaos in the nonlinear schrödinger equation. *Contemporary Mathematics*, 172:253–268, 1994.
- [7] M. J. Ablowitz, C. M. Schober, and B. M. Herbst. Numerical chaos, roundoff errors and homoclinic manifolds. *Physical Review Letters*, 71(17):2683–2686, October 1993.
- [8] M. J. Ablowitz and H. Segur. *Solitons and the Inverse Scattering Transform*. Number 4 in SIAM Studies in Applied Mathematics. SIAM, 1981.
- [9] D. Cai, A. R. Bishop, N. Grønbech-Jensen, and M. Salerno. Electric field-induced nonlinear bloch oscillations and dynamical localization. *Physical Review Letters*, 74:1186, 1995.
- [10] J. C. Eilbeck, P. S. Lombdahl, and A. C. Scott. The discrete self-trapping equation. *Physica*, 16 D:318–338, 1985.
- [11] S. G. Evangelides, L. F. Mollenauer, J. P. Gordon, and N. S. Bergano. Polarization multiplexing with solitons. *Journal of Lightwave Technology*, 10(1):28–35, January 1992.
- [12] B. M. Herbst and M. J. Ablowitz. Numerical chaos, symplectic integrators and exponentially small splitting distances. *Journal of Computational Physics*, 105:122–132, 1993.
- [13] V. M. Kenkre and D. K. Campbell. Self-trapping on a dimer: time-dependent solutions of a discrete nonlinear Schrödinger equation. *Physical Review B*, 34:4959–4961, 1986.
- [14] V. M. Kenkre and G. P. Tsironis. Nonlinear effects in quasilinear neutron scattering: exact line calculation for a dimer. *Physical Review B*, 35:1473–1484, 1987.
- [15] T. I. Lakoba and D. J. Kaup. Perturbation theory for the manakov soliton and its applications to pulse propagation in randomly birefringent fibers. *Physical Review E*, 56(5):6147–6165, November 1997.
- [16] S. V. Manakov. On the theory of two-dimensional stationary self-focusing of electromagnetic waves. *Soviet Physics JETP*, 38(2):248–253, 1974.
- [17] D. W. McLaughlin and E. A. Overman II. *Surveys in Applied Mathematics*, volume 1, chapter Whiskered Tori for Integrable Pde’s: Chaotic behavior in near Integrable Pde’s. Plenum Press, New York, 1995.
- [18] C. R. Menyuk. Nonlinear pulse propagation in birefringent optical fibers. *IEEE Journal of Quantum Electronics*, QE-23(2):174–176, February 1987.

- [19] C. R. Menyuk. Pulse propagation in an elliptically birefringent Kerr medium. *IEEE Journal of Quantum Electronics*, 25(12):2674–2682, December 1989.
- [20] Y. Ohta. Pfaffian solutions for coupled discrete nonlinear schrödinger equation. *Chaos, Solitons and Fractals*, to appear. Proceedings of Brussels Meeting II: Integrability and Chaos in Discrete Systems (Brussels, 2-6 July 1997).
- [21] V. S. Shchesnovich and E. V. Doktorov. Perturbation theory for solitons of the Manakov system. *Physical Review E*, 55(6):7626–7635, June 1997.
- [22] Y. B. Suris. A discrete-time Garnier system. *Physics Letters. A*, 189(4):281–289, 1994.

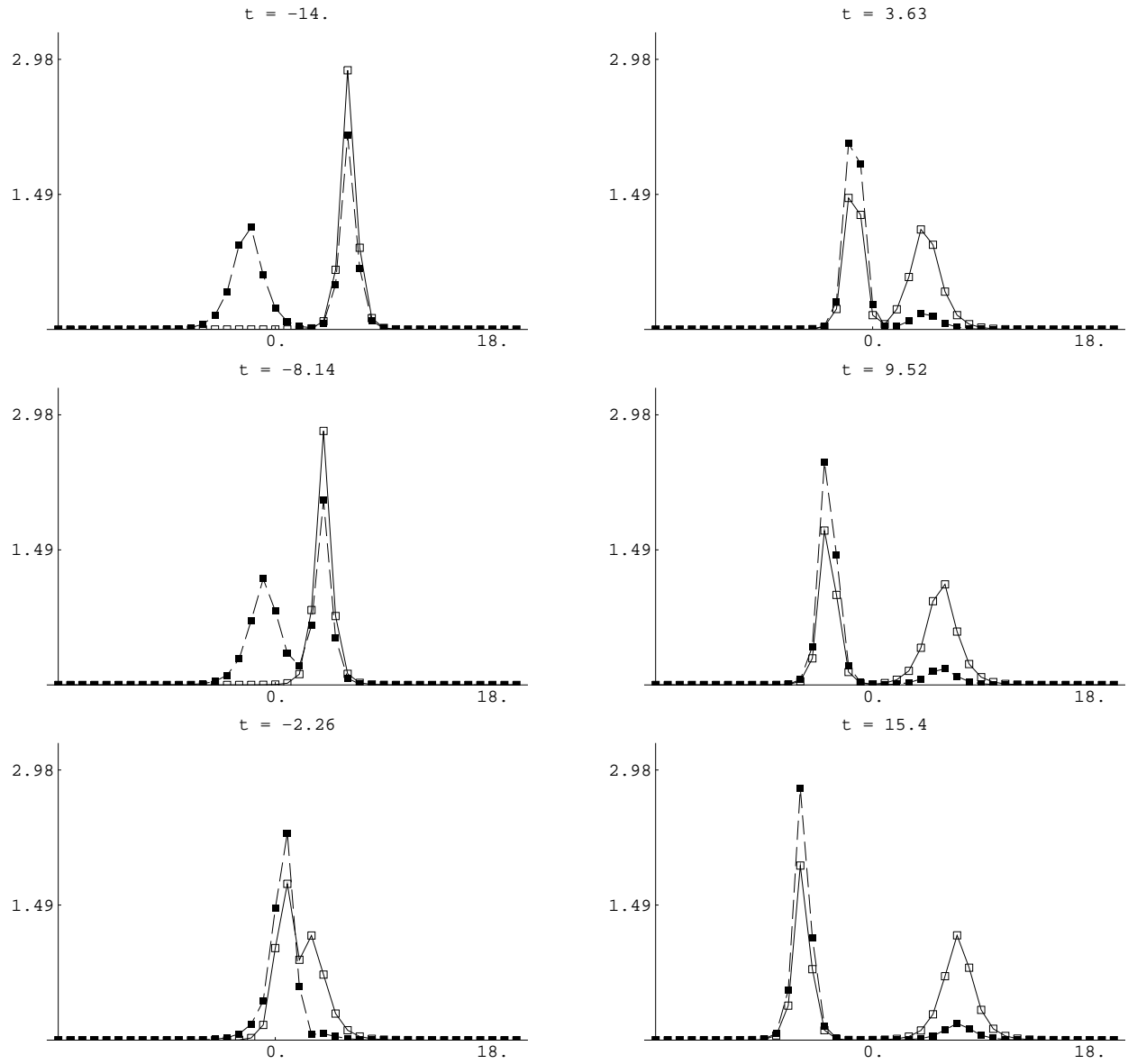


Figure 1: Two-soliton interaction for the symmetric system. The filled boxes are $|q_n^{(1)}|$ and the open boxes are $|q_n^{(2)}|$. Increasing time is read down column-wise. Soliton 1 is on the left and Soliton 2 is on the right at $t = -14$. They are reversed at $t = 15.4$. The soliton parameters are: $a_1 = 1$, $a_2 = 2$, $b_1 = .1$, $b_2 = -.1$. The polarization vectors are: $\mathbf{c}_1^- = (1, 0)$, $\mathbf{c}_2^- = (.6e^{i\pi/3}, .8)$, at $t = -14$, and $\mathbf{c}_1^+ = (.16e^{i.58\pi}, .98e^{-i.16\pi})$, $\mathbf{c}_2^+ = (.82e^{i.27\pi}, .57e^{-i.03\pi})$ at $t = 15.4$. This is a typical two-soliton interaction where $0 < |\mathbf{c}_1^- \cdot \mathbf{c}_2^-| = .6 < 1$, $|\mathbf{c}_1^- \cdot \mathbf{c}_1^+| = .16 < 1$ and $|\mathbf{c}_2^- \cdot \mathbf{c}_2^+| = .95 < 1$.

tol	Error: $\log_{10} \Delta_j$	
	soliton 1	soliton 2
10^{-6}	-4.11	-5.97
10^{-7}	-5.33	-6.99
10^{-8}	-6.58	-8.00
10^{-9}	-7.84	-9.01
10^{-10}	-9.12	-10.0

Table 1: Difference between solution at the final time and a soliton wave-form for a two solitary-wave interaction. Soliton parameters: $a_1 = 2$, $b_1 = 0.1$, $\mathbf{c}_1^- = (1, 0)$, $a_2 = 1$, $b_2 = -0.1$, $\mathbf{c}_2^- = (\frac{1}{\sqrt{2}}, \frac{1}{\sqrt{2}})$. “ tol ” is the error tolerance allowed by the NAG routine D02BAF. The errors in the table are the \log_{10} of the error given by (26). The error decreases proportionally with the error tolerance used in the simulation. This indicates that the errors are due to the time integration and that, therefore, the solitary waves interact as solitons.

\mathbf{c}_2^-	$ \mathbf{c}_1^- \cdot \mathbf{c}_1^+ $	$ \mathbf{c}_2^- \cdot \mathbf{c}_2^+ $	\mathbf{c}_2^-	$ \mathbf{c}_1^- \cdot \mathbf{c}_1^+ $	$ \mathbf{c}_2^- \cdot \mathbf{c}_2^+ $
$(0.2e^{i0}, .98e^{i0})$	0.843	0.985	$(0.2e^{i\pi/3}, .98e^{i0})$	0.843	0.985
$(0.4e^{i0}, .92e^{i0})$	0.465	0.958	$(0.4e^{i\pi/3}, .92e^{i0})$	0.465	0.958
$(0.6e^{i0}, 0.8e^{i0})$	0.158	0.947	$(0.6e^{i\pi/3}, 0.8e^{i0})$	0.158	0.947
$(0.8e^{i0}, 0.6e^{i0})$	0.544	0.962	$(0.8e^{i\pi/3}, 0.6e^{i0})$	0.544	0.962
$(0.2e^{i\pi/2}, .98e^{i0})$	0.843	0.985	$(0.2e^{i\pi}, .98e^{i0})$	0.843	0.985
$(0.4e^{i\pi/2}, .92e^{i0})$	0.465	0.958	$(0.4e^{i\pi}, .92e^{i0})$	0.465	0.958
$(0.6e^{i\pi/2}, 0.8e^{i0})$	0.158	0.947	$(0.6e^{i\pi}, 0.8e^{i0})$	0.158	0.947
$(0.8e^{i\pi/2}, 0.6e^{i0})$	0.544	0.962	$(0.8e^{i\pi}, 0.6e^{i0})$	0.544	0.962

Table 2: Shift in polarization in the two-soliton interaction of the symmetric system. The soliton parameters are $a_1 = 1$, $a_2 = 2$, $b_1 = .1$, $b_2 = -.1$. The polarizations before interaction are $\mathbf{c}_1^- = (1, 0)$ and \mathbf{c}_2^- as given in the table. The polarizations after interaction are \mathbf{c}_1^+ and \mathbf{c}_2^+ . The values $|\mathbf{c}_j^- \cdot \mathbf{c}_j^+| < 1$ indicate that the polarization vectors are shifted by the soliton interaction. These results were obtained by numerical simulation.